

AN ULTRAMASSIVE 1.28 M_⊙ WHITE DWARF IN NGC 2099¹

JEFFREY D. CUMMINGS², JASON S. KALIRAI^{3,2}, P.-E. TREMBLAY⁴, ENRICO RAMIREZ-RUIZ⁵, AND P. BERGERON⁶

Draft version April 30, 2018

ABSTRACT

With the Keck I Low-Resolution Imaging Spectrometer we have observed nine white dwarf candidates in the very rich open cluster NGC 2099 (M37). The spectroscopy shows seven to be DA white dwarfs, one to be a DB white dwarf, and one to be a DZ white dwarf. Three of these DA white dwarfs are consistent with singly evolved cluster membership: an ultramassive ($1.28_{-0.08}^{+0.05}$ M_⊙) and two intermediate-mass (0.70 and 0.75 M_⊙) white dwarfs. Analysis of their cooling ages allows us to calculate their progenitor masses and establish new constraints on the initial-final mass relation. The intermediate-mass white dwarfs are in strong agreement with previous work over this mass regime. The ultramassive white dwarf has $V = 24.5$, ~ 2 mag fainter than the other two remnants. The spectrum of this star has lower quality, so the derived stellar properties (e.g., T_{eff} , $\log g$) have uncertainties that are several times higher than the brighter counterparts. We measure these uncertainties and establish the star's final mass as the highest-mass white dwarf discovered thus far in a cluster, but we are unable to calculate its progenitor mass because at this high mass and cooler T_{eff} its inferred cooling age is highly sensitive to its mass. At the highest temperatures, however, this sensitivity of cooling age to an ultramassive white dwarf's mass is only moderate. This demonstrates that future investigations of the upper-mass end of the initial-final mass relation must identify massive, newly formed white dwarfs (i.e., in young clusters with ages 50-150 Myr).

1. INTRODUCTION

White dwarfs that are members of well-studied star clusters are extremely valuable for understanding the process of stellar evolution and mass loss. The progenitor masses (hereafter M_{initial}) of these white dwarfs can be calculated by comparing the remnant's cooling age to the cluster age, a technique that has now led to a well established initial-final mass relation (IFMR) from $M_{\text{initial}} = 0.8$ to 5 M_⊙ (e.g., Claver et al. 2001; Dobbie et al. 2004, 2006a; Williams et al. 2004; Kalirai et al. 2005; Liebert et al. 2005; Williams & Bolte 2007; Kalirai et al. 2007; Kalirai et al. 2008; Rubin et al. 2008; Kalirai et al. 2009; Williams et al. 2009; Dobbie et al. 2012; Cummings et al. 2015, hereafter Paper I; Cummings et al. 2016, hereafter Paper II). At higher white dwarf masses (hereafter M_{final}), the relation remains poorly constrained. The progenitors of these massive white dwarfs are intermediate-mass stars that quickly evolve to asymptotic giant branch (AGB) stars, which lose mass through dust driven outflows and thermal pulses. This phase of stellar evolution is poorly understood from first

principles and is difficult to model through direct observations. New constraints on the IFMR in this regime would be a breakthrough for stellar astrophysics.

Finding and characterizing high-mass white dwarfs is longstanding challenge due to their scarcity. In the Sloan Digital Sky Survey and Palomar Green Survey only 1.5% and 2.6%, respectively, of the field white dwarfs have a $M_{\text{final}} \geq 1.05$ M_⊙ (e.g., Kleinman et al. 2013; Kepler et al. 2016; Liebert et al. 2005). In star clusters their number remains limited at six. A long known high-mass white dwarf is LB 1497 from the young Pleiades star cluster at 1.05 M_⊙ (Gianninas et al. 2011). The remaining five have been recently discovered: NGC 2287-4 (Dobbie et al. 2012), NGC 2168-LAWDS27 (Williams et al. 2009), two white dwarfs in NGC 2323 (Paper II), and VPHASJ1103-5837 in NGC 3532 (Raddi et al. 2016). VPHASJ1103-5837 has a $M_{\text{final}} \sim 1.13$ M_⊙ and the four others all have a $M_{\text{final}} \sim 1.07$ M_⊙ (Paper II). Two special cases are GD50 at 1.25 ± 0.02 M_⊙ and PG 0136+251 at 1.19 ± 0.03 M_⊙, which are ultramassive white dwarfs with possible connection to the Pleiades. Based on GD50's space motion, Dobbie et al. (2006b) find a high probability it is coeval with the young Pleiades and that it was ejected from the cluster. Similar analysis of PG 0136+251 finds provisional connections to the Pleiades based on its proper motion, but its radial velocity is still needed to verify this connection (Dobbie et al. 2006b). The scarcity of massive white dwarfs in the Galactic field, but even more so in stellar clusters, has led to arguments that most massive white dwarfs are formed through mass transfer or white dwarf mergers, which theoretically can form such massive white dwarfs (e.g., Dan et al. 2014). These merger processes may create excess massive white dwarfs in the field but would not yet play a significant role in the younger cluster populations.

¹ Based on observations with the W.M. Keck Observatory, which is operated as a scientific partnership among the California Institute of Technology, the University of California, and NASA, was made possible by the generous financial support of the W.M. Keck Foundation.

² Center for Astrophysical Sciences, Johns Hopkins University, Baltimore, MD 21218, USA; jcummi19@jhu.edu

³ Space Telescope Science Institute, 3700 San Martin Drive, Baltimore, MD 21218, USA; jkalirai@stsci.edu

⁴ Department of Physics, University of Warwick, Coventry CV4 7AL, UK; P-E.Tremblay@warwick.ac.uk

⁵ Department of Astronomy and Astrophysics, University of California, Santa Cruz, CA 95064; enrico@ucolick.org

⁶ Département de Physique, Université de Montréal, C.P. 6128, Succ. Centre-Ville, Montréal, QC H3C 3J7, Canada; bergeron@ASTRO.UMontreal.CA

There are several reasons, however, that can explain this scarcity besides the challenge that their progenitors ($M_{\text{initial}} > 6 M_{\odot}$) are rare. These include that: (1) Increasingly higher-mass white dwarfs become more compact under their strong gravities, which gives them significantly smaller radii and luminosity in comparison to their lower-mass companions. (2) These white dwarfs form from rapidly evolving higher-mass stars, which means that in most clusters they have already undergone significant cooling, further limiting their visibility. (3) High-mass white dwarfs may be prone to be ejected from their parent clusters, either due to dynamical interactions or velocity kicks resulting from asymmetric mass loss during their formation (Fellhauer et al. 2003; Tremblay et al. 2012).

Our search for ultramassive white dwarfs begins with the very rich NGC 2099 with a large population of 50 white dwarf candidates (e.g., Kalirai et al. 2001; 2005; Paper I). In Paper I we spectroscopically confirmed the white dwarf nature of 19 of the brighter white dwarf candidates in the cluster and measured their masses. That work set the bulk of the constraints on the intermediate mass range of the IFMR (e.g., $M_{\text{initial}} = 2.5$ to $4.0 M_{\odot}$). In this letter, we push the initial study to fainter luminosities in search of more massive white dwarfs.

In Section 2 we discuss the spectroscopic white dwarf observations of NGC 2099 and describe the reduction and analysis techniques. In Section 3 we discuss the cluster membership of the white dwarf candidates in NGC 2099. In Section 4 we look at the M_{initial} and M_{final} of each white dwarf cluster member and analysis in detail the errors of ultramassive white dwarfs. In Section 5 we summarize our results.

2. OBSERVATIONS, REDUCTIONS & ANALYSIS

Our previous Keck I Low Resolution Imaging Spectrometer (LRIS; Oke et al. 1995) observations of NGC 2099, presented in Paper I, observed a faint candidate (WD33) at $V = 24.49 \pm 0.065$. The resulting WD33 spectrum was not suitable for publication, but it suggested that this faint white dwarf had a high mass. We obtained new Keck/LRIS observations during 2015 February 18 and 19 with a slitmask to re-observe WD33 and eight new white dwarf candidates in NGC 2099. These additional eight targets span V from 22.3 to 24.3 and were selected based on the 11 white dwarfs in Paper I that were found to be consistent with NGC 2099 membership. Five hours of observation were acquired on this mask.

Continuing with the methods from Paper I and II, we reduced and flux calibrated the new LRIS observations using the IDL based XIDL pipeline⁷. Of the total observed sample of nine white dwarf candidates, seven are DA white dwarfs, one is a DB white dwarf, and one is a DZ white dwarf. The new observations of WD33 have been coadded to the original observations taken with Keck/LRIS under the same configuration.

For the spectroscopic DA analysis, we adopted the same techniques as described in Paper II but with updated oxygen/neon (ONe) white dwarf models. In brief, we used the white dwarf spectroscopic models of Tremblay et al. (2011) with the Stark profiles of Tremblay &

Bergeron (2009), and the automated fitting techniques from Bergeron et al. (1992) to fit the Balmer line spectra and derive T_{eff} and $\log g$. For the spectroscopic DB analysis, we adopted the methods in Bergeron et al. (2011). For deriving M_{final} , luminosity, and cooling age of the lower mass ($< 1.10 M_{\odot}$) DA white dwarfs and the DB white dwarf, the cooling models by Fontaine et al. (2001) were used for a carbon/oxygen (CO) core composition with a thick and thin hydrogen layer, for hydrogen and helium atmospheres, respectively. Lastly, for massive white dwarfs up to $1.28 M_{\odot}$ we derived M_{final} , luminosity, and cooling age based on the ONe-core models of Althaus et al. (2007), up to $1.38 M_{\odot}$ we used unpublished ultramassive models using consistent physics (L.G. Althaus; private communication 2016). This both expands the mass range and updates our adopted ONe mass-radius relationship to that from the Althaus et al. (2007) models. In contrast, the Paper II analysis used the older mass-radius relationship from Althaus et al. (2005).

Table 1 presents the observed and derived parameters for the new white dwarf candidates from NGC 2099. We have organized these white dwarfs by type and membership (see Section 3), but we also separate the DZ WD26 because we cannot analyze it and WD30, WD31, and WD32 because they have very low S/N spectra with mass uncertainties $> 0.1 M_{\odot}$. Their membership analysis is unreliable so we did not use them in the IFMR.

Table 1 also includes the newly discovered VPHASJ1103-5837 from NGC 3532 (Raddi et al. 2016) and updated initial and final-masses for GD50 and PG 0136+251 (Gianninas et al. 2011). The spectroscopic analysis techniques in both studies were equivalent to ours, so we applied their T_{eff} and $\log g$ directly (we added external errors [see Paper I] to VPHASJ1103-5837's published errors), and we derived both the masses and cooling ages from the ONe models of Althaus et al. (2007).

3. WHITE DWARF MEMBERSHIP IN NGC 2099

To apply these white dwarfs to the IFMR, cluster membership must be verified to be able to infer their M_{initial} . For WD33, the significant mass and high T_{eff} is by itself a strong argument for membership, but to refine its membership and determine the membership status of the other observed white dwarfs we compared the predicted colors and magnitudes to the photometry (see Table 1). This is similar to the procedure from Paper I, where we compared to the NGC 2099 photometry from Kalirai et al. (2001), but we now have an expanded sample and color range to both refine the white dwarf based distance modulus and reddening and to also look for trends with color.

Figure 1 compares the apparent distance moduli and reddenings for each observed white dwarf with sufficient signal and plots them versus their model-based predicted color. Their 1σ distance modulus and reddening errors are shown, which are the photometric and model-based errors added in quadrature. In both cases, we find color trends for distance modulus and reddening. These trends may be the result of the photometric standardization, which can be less precise in both blue stars and in faint stars. Additionally, the reddening in NGC 2099 is quite large, and as discussed in Paper I (see also Fernie et al.

⁷ Available at <http://www.ucolick.org/~xavier/IDL/>

TABLE 1 - White Dwarf Initial & Final Parameters

ID	M_V	B- V_0	V	B-V	α	δ	T_{eff}	log g	M_{final}	t_{cool}	M_{initial}	S/N
	Model		Obs		(J2000)	(J2000)	(K)		(M_{\odot})	(Myr)	(M_{\odot})	
Likely DA White Dwarf Members of NGC 2099												
WD25	10.31	-0.18	22.30	0.16	05:52:44.44	+32:29:54.7	27500±450	8.11±0.06	0.70±0.03	17 ⁺⁵ ₋₃	2.95 ^{+0.01} _{-0.01} ^{+0.10} _{-0.10}	82
WD28	10.89	-0.09	22.73	0.20	05:52:44.37	+32:25:22.4	22000±400	8.20±0.06	0.75±0.03	76 ⁺¹³ ₋₁₂	3.07 ^{+0.03} _{-0.03} ^{+0.13} _{-0.11}	76
WD33	12.29	-0.31	24.49	0.07	05:52:36.35	+32:27:16.8	32900±1100	9.27±0.22	1.28 ^{+0.05} _{-0.08}	233 ⁺¹⁰² ₋₁₁₈	3.58 ^{+0.62} _{-0.41} ^{+0.25} _{-0.20}	22
DA White Dwarf Inconsistent with Single Star Membership of NGC 2099												
WD29	11.41	0.01	23.13	0.41	05:53:04.82	+32:29:26.0	17300±500	8.26±0.10	0.77±0.06	195 ⁺³⁹ ₋₃₄	—	36
DB White Dwarf in the field of NGC 2099												
WD27	11.68	-0.07	22.60	0.14	05:52:45.31	+32:25:49.4	22100±120	8.66±0.07	1.01±0.05	204 ⁺⁴⁶ ₋₄₀	—	67
Low Signal to Noise DA White Dwarfs and a DZ White Dwarf in the field of NGC 2099												
WD30	11.26	-0.02	23.66	0.28	05:53:03.06	+32:26:12.4	18200±950	8.22±0.16	0.75±0.11	158 ⁺⁶³ ₋₅₀	—	18
WD31	11.06	0.06	24.26	0.35	05:52:53.69	+32:30:11.3	14400±1200	7.80±0.21	0.50±0.11	165 ⁺⁸² ₋₅₇	—	20
WD32	11.04	-0.09	24.34	0.26	05:53:01.44	+32:26:42.0	22400±2000	8.31±0.28	0.82±0.17	94 ⁺⁸² ₋₅₇	—	12
WD26	—	—	22.44	0.36	05:53:07.18	+32:28:59.9	—	—	—	—	—	50
Massive white dwarf members of NGC 3532 and the Pleiades.												
VPHASJ1103-5837					11:03:58.00	-58:37:09.2	23900±450	8.87±0.06	1.11±0.03	223 ⁺⁴⁰ ₋₃₀	5.40 ^{+1.36} _{-0.55}	35
GD50					03:46:17.26	-01:07:31.5	42700±800	9.20±0.07	1.26±0.02	76 ⁺¹⁷ ₋₁₁	6.41 ^{+0.72} _{-0.41}	—
PG 0136+251					01:38:53.02	+25:23:22.8	41400±800	9.03±0.07	1.20±0.03	52 ⁺¹⁴ ₋₁₂	5.78 ^{+0.48} _{-0.32}	—

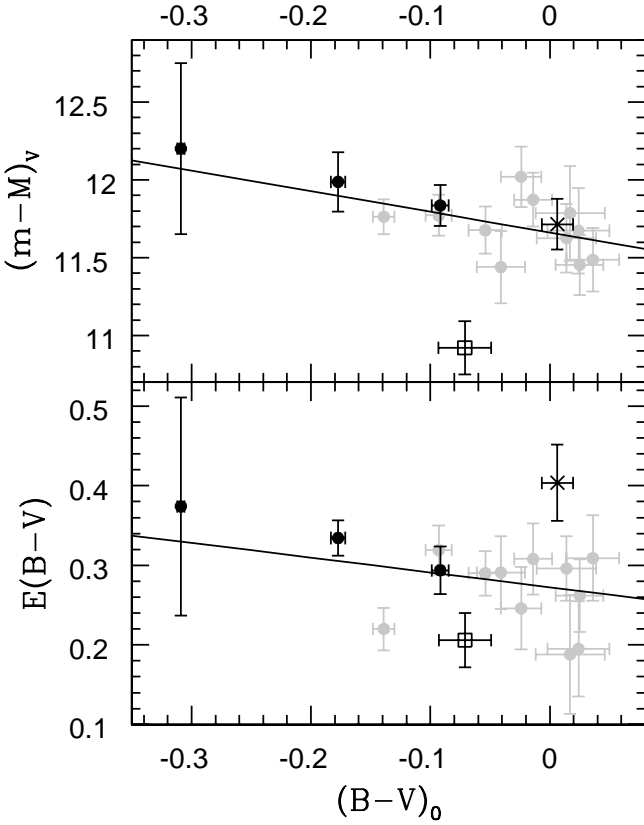
 TABLE 1 The first M_{initial} errors are based on the white dwarf parameter errors and for NGC 2099 members the second M_{initial} errors are based on cluster age errors.


FIG. 1.— The upper panel shows the effective distance modulus for the DA members (solid black) and nonmember (x), and the DB white dwarf (open square). The data are plotted versus predicted $(B-V)_0$ and are compared to the NGC 2099 members from Paper I (solid gray). The lower panel shows the effective reddening versus predicted $(B-V)_0$. The solid lines illustrate the color trends for distance modulus and reddening. All white dwarfs are plotted with their 1σ error bars, and white dwarfs within 2σ of the trend in both distance modulus and reddening are considered members.

1963) at reddenings $E(B-V) > 0.2$ the effective reddening and extinction are meaningfully dependent on intrinsic

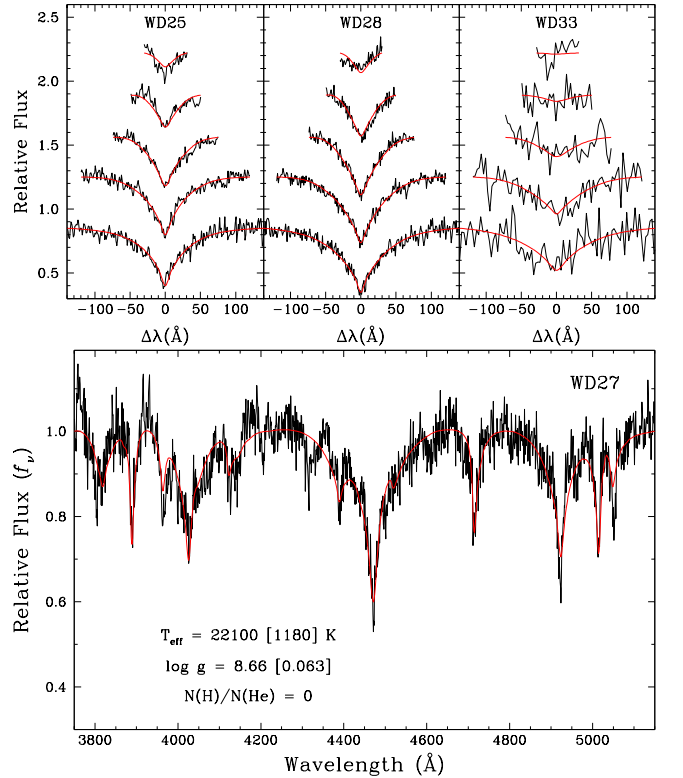


FIG. 2.— The upper three panels show the Balmer line fits for the three white dwarf members of NGC 2099. The spectrum of WD33 has been binned for display purposes. The $H\beta$, $H\gamma$, $H\delta$, $H\epsilon$, and $H8$ fits are shown from bottom to top. The lower panel shows the fit of WD27's He features, where we have adopted a pure He atmosphere.

color. We find WD25, WD28, and WD33 are consistent with single star membership in NGC 2099 because they are within 2σ of the trend in both distance modulus and reddening.

The observed photometry of the DB white dwarf

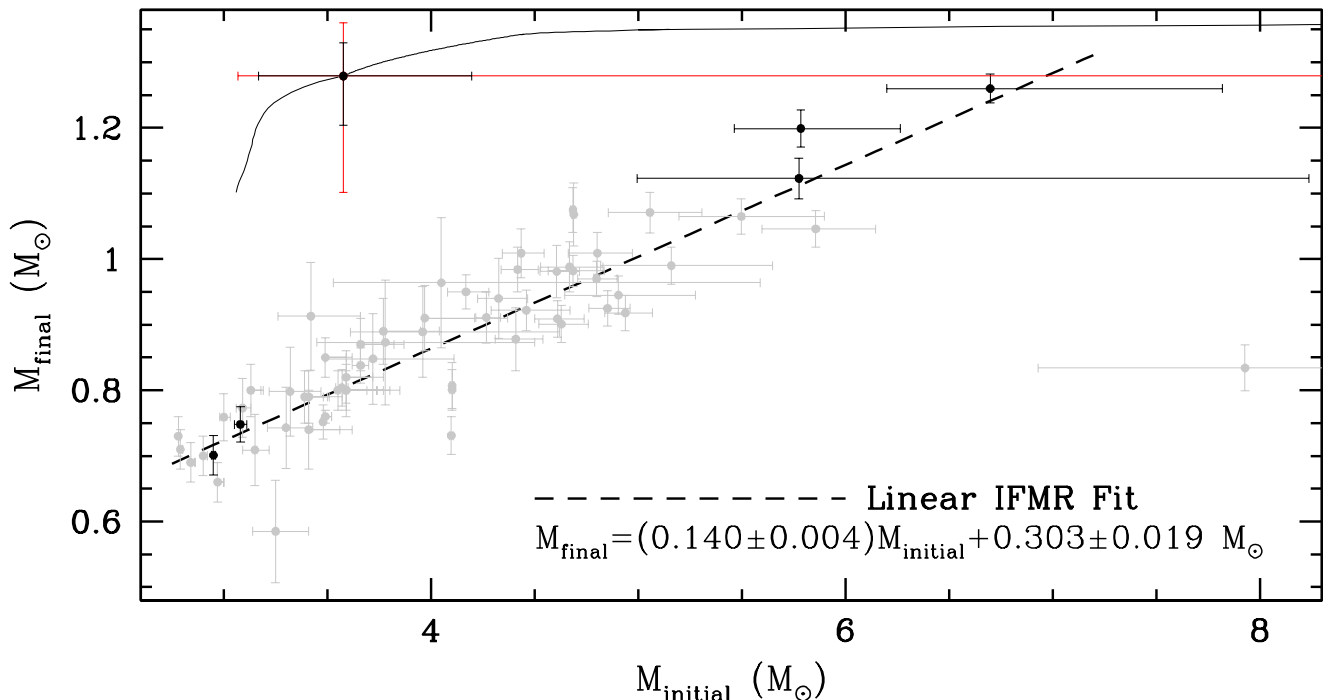


FIG. 3.— The IFMR data from Paper I and II (gray) are plotted with the three newly observed members of NGC 2099 (black). WD25 and WD28 are strongly consistent with the previous data, while the ultramassive WD33 gives a very low M_{initial} but with significant mass errors (1σ -black; 2σ -red). Because the initial and final mass errors in WD33 are not independent, we also display a curve showing the direct and strong relation between adopted M_{final} and the resulting M_{initial} . We also include VPHASJ1103-5837 and the updated Pleiades white dwarfs. The fit relation displayed does not consider WD33 due to its significant errors.

WD27 is 0.84 ± 0.17 magnitudes too bright to be consistent with single star membership. However, if it is a binary member of two comparable luminosity white dwarfs its observed magnitude would be ~ 0.75 magnitudes brighter than the model predicts. The inferred reddening of this DB white dwarf is $\sim 2\sigma$ lower than expected for a member, which may suggest it is a less-reddened foreground DB white dwarf, but it is still within the reddening membership criterion. Additionally, its younger cooling age of 204 Myr is well within the NGC 2099 cluster age of 520 ± 50 Myr (Kalirai et al. 2001; Paper I). However, we note the unlikelihood of a binary with two nearly equivalent DB white dwarfs and the lack of Balmer features in the spectrum (see Figure 2) that would indicate a DA companion. Irrespective of membership, WD27 is an interesting and very rare DB because it is both moderately hot and high mass (see Bergeron et al. 2011; Koester & Kepler 2015).

Figure 2 displays the spectral fits of the three white dwarf members WD25, WD28, and WD33, and the DB white dwarf WD27. While the WD33 spectrum has low S/N, most notably at the two highest-order Balmer lines, at this high mass and moderate T_{eff} these highest-order lines become increasingly less sensitive to $\log g$. For example, fitting only the first four Balmer lines derives $\log g = 9.23 \pm 0.22$ and only the first three lines derives $\log g = 9.30 \pm 0.24$. Lastly, spectral analysis of 831 synthetic spectra with input parameters of $T_{\text{eff}} = 32,900$ K and $\log g = 9.27$ and $S/N = 22$ finds a normally distributed series of $\log g$ measurements with a mean consistent with the input, and the distribution's σ matches our spectral analysis's fitting error.

4. INITIAL-FINAL MASS RELATION

We measured the IFMR by comparing each white dwarf's cooling age to the NGC 2099 cluster age (520 Myr). The difference between these ages gives the evolutionary time to the tip of the AGB for each white dwarf's progenitor. We applied these times to the PARSEC evolutionary models (Bressan et al. 2012) to determine each white dwarf's M_{initial} . These M_{initial} values are given in Table 1, including two M_{initial} errors based on the white dwarf parameter errors and from the cluster age errors (520 ± 50 Myr). For the M_{initial} of VPHASJ1103-5837 we adopted for NGC 3532 the Paper II cluster age of 320 Myr. For GD50 and PG 0136+251 we adopted for Pleiades the Paper II cluster age of 135 Myr.

Beginning with the high-mass DB white dwarf WD27, if WD27 is a double degenerate consistent with cluster membership it may have undergone some level of binary interaction in its past. This could potentially explain its nature, but this would also make its inferred M_{initial} unreliable. Testing this, its relatively short cooling time of 204_{-34}^{+39} Myr implies a M_{initial} of only $3.46_{-0.12}^{+0.16} M_{\odot}$, while our IFMR fit gives that a singly evolved $1.0 M_{\odot}$ white dwarf would have a $\sim 5.0 M_{\odot}$ progenitor.

Figure 3 compares the Paper I and II IFMR data with VPHASJ1103-5837, the updated Pleiades white dwarfs, and the three newly observed NGC 2099 members. WD25, WD28, VPHASJ1103-5837, PG 0136+251, and GD50 are strongly consistent with the Paper II IFMR trend. The ultramassive WD33, however, is very discrepant, but there are several possible explanations for this. First, is it a supermassive white dwarf formed through a merger of two lower-mass white dwarfs? Based on the models of white dwarf mergers from Dan et al. (2014), the mechanism to create a stable supermassive

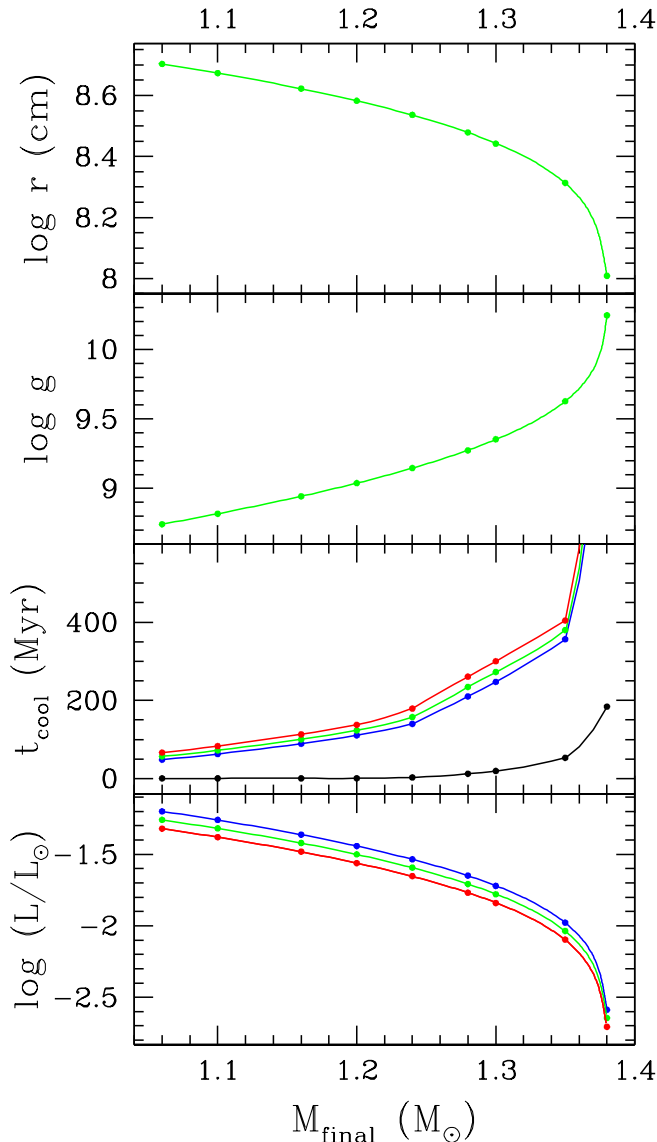


FIG. 4.— These panels illustrate how log radius, log g , cooling age, and $\log L/L_{\odot}$ vary with M_{final} at constant T_{eff} in the ONE models of Althaus et al. (2007) plus consistent higher-mass models. Green represents the derived T_{eff} of WD33 at 32,900 K. The lower two panels illustrate the effects of the ± 1100 K T_{eff} errors by plotting 34,000 K (blue) and 31,800 K (red). The cooling age at 1.38 M_{\odot} is not displayed but is 1168^{+114}_{-101} Myr. For cooling age, we also illustrate the weakened sensitivity to mass at a higher T_{eff} of 65,000 K (black).

white dwarf requires the merging of two comparable white dwarfs of approximately half its mass ($\sim 0.64 M_{\odot}$). Based on the age of NGC 2099 this is pushing the minimum mass of a white dwarf that could have formed after 520 Myr. Binary interactions could have affected their evolutionary timescales, but they still would have likely just formed in the recent past and would not have had the time to both merge to create WD33 and subsequently cool for 233 Myr.

Second, WD33 could be the result of a binary merger event that occurred while the components were still evolving. Two binary components of both $\sim 3.5 M_{\odot}$ could have undergone interaction and subsequent merger. This would have created a short-lived $\sim 7 M_{\odot}$ blue straggler that quickly formed into WD33 and had sufficient

time to still cool for 233 Myr.

Lastly, another possibility relates to both the analysis and systematic errors in the ONE cooling models themselves. The errors in black in Figure 3 are the 1σ errors in both M_{final} and M_{initial} . Expanding our error analysis in WD33 to look at 2σ variations in $\log g$ (in red) finds that at higher masses the uncertainty in the cooling age rapidly expands. This results from a white dwarf’s radius becoming increasingly sensitive to mass in this regime (Althaus et al. 2005; 2007). Figure 4 displays the Althaus et al. (2007) mass-radius relationship at WD33’s T_{eff} of 32,900 K. This mass sensitivity in radius also leads to a significant sensitivity in $\log g$, cooling age, and luminosity at higher masses. In Figure 4, we also analyze the sensitivity to WD33’s 1σ T_{eff} error (1100 K) for cooling age and luminosity, with a high- T_{eff} (blue) and low- T_{eff} (red) curve. This illustrates that at the highest masses the sensitivity of the cooling age to T_{eff} errors is minor relative to the mass dependence.

In application to the ultramassive IFMR, one advantage of these strong dependencies is that large errors in the spectroscopically derived $\log g$ result in only moderate to minor errors in M_{final} . A second advantage is that the increasing sensitivity of luminosity to M_{final} can be used to independently infer mass from photometry, but uncertainties in WD33’s observed magnitude and NGC 2099’s visual distance modulus currently limit how accurately we can observationally derive its M_V .

The significant challenge for the ultramassive IFMR is the extreme sensitivity to M_{final} of cooling age, and hence M_{initial} . As seen in Table 1 and Figure 4, WD33’s parameters only derive a modest cooling age of 233 Myr, and with the adopted cluster age of 520 Myr this gives a very low M_{final} of 3.58 M_{\odot} . A 1σ increase in WD33’s mass to 1.33 M_{\odot} increases the derived cooling age to 331 Myr. While a 2σ increase in white dwarf mass, from propagating a 2σ increase in $\log g$, to 1.36 M_{\odot} increases the cooling age to 546 Myr, surpassing the cluster age. Figure 3 demonstrates this strong dependence of initial and final mass errors with a single curve passing through WD33. This also illustrates the additional challenge that as M_{initial} increases the sensitivity of derived M_{initial} to evolutionary lifetime increases rapidly.

These cooling age challenges, reassuringly, do not equally affect all ultramassive white dwarfs. The youngest and hottest white dwarfs in this mass range are significantly less susceptible to these complications (e.g., GD50). First, these young white dwarfs are higher luminosity, increasing the ease of acquiring high-signal spectra. Second, the sensitivity of cooling age on white dwarf mass significantly decreases at high T_{eff} . For example, at WD33’s T_{eff} of 32,900 K, a decrease in M_{final} from 3.36 to 3.34 M_{\odot} causes a 191 Myr decrease in inferred cooling age. For a young white dwarf at T_{eff} of 65,000 K, this same change in M_{final} would result in a decrease in inferred cooling age of 37 Myr (see full comparison in Figure 4). A third advantage for young and ultramassive white dwarfs is that cooling ages are further complicated by dependencies on both the input physics and composition in the adopted cooling model, where potential systematics introduced in the cooling age grow rapidly with increasing cooling age.

5. SUMMARY

We have observed nine new white dwarf candidates in NGC 2099. Two intermediate-mass (WD25, WD28) and one ultramassive (WD33) DA white dwarfs were found to be consistent with membership. We also compared to the self-consistently analyzed GD50, PG 0136+251, and the newly discovered VPHASJ1103-5837. Application of these data to the IFMR finds strong consistency with our previous work for all but WD33, but this may be explained by WD33's significant M_{initial} errors. Acquiring additional spectroscopic signal on WD33 may be of interest, and more accurate photometry would also be useful, but overcoming these errors at this mass and T_{eff} currently may not be viable at $V=24.49$. For precise application of ultramassive white dwarfs to the IFMR, future studies should focus on clusters of age ~ 50 to 150

Myr. Nevertheless, because GD50 and PG 0136+251 are only kinematically connected to the Pleiades, WD33 is the first ultramassive white dwarf that is photometrically consistent with membership in a star cluster.

This project was supported by the National Science Foundation (NSF) through grant AST-1211719. This work was also supported by a NASA Keck PI Data Award, administered by the NASA Exoplanet Science Institute. Data presented herein were obtained at the WM Keck Observatory from telescope time allocated to the National Aeronautics and Space Administration through the agency's scientific partnership with the California Institute of Technology and the University of California. The Observatory was made possible by the generous financial support of the WM Keck Foundation.

REFERENCES

- Claver, C. F., Liebert, J., Bergeron, P., & Koester, D. 2001, *ApJ*, 563, 987
- Bergeron, P., Saffer, R. A., & Liebert, J. 1992, *ApJ*, 394, 228
- Bergeron, P., Wesemael, F., Dufour, P., et al. 2011, *ApJ*, 737, 28
- Bressan, A., Marigo, P., Girardi, L., et al. 2012, *MNRAS*, 427, 127
- Cummings, J. D., Kalirai, J. S., Tremblay, P.-E., & Ramirez-Ruiz, E. 2015, *ApJ*, 807, 90
- Cummings, J. D., Kalirai, J. S., Tremblay, P.-E., & Ramirez-Ruiz, E. 2016, *ApJ*, 818, 84
- Dan, M., Rosswog, S., Brüggen, M., & Podsiadlowski, P. 2014, *MNRAS*, 438, 14
- Dobbie, P. D., Pinfield, D. J., Napiwotzki, R., et al. 2004, *MNRAS*, 355, L39
- Dobbie, P. D., Napiwotzki, R., Burleigh, M. R., et al. 2006a, *MNRAS*, 369, 383
- Dobbie, P. D., Napiwotzki, R., Lodieu, N., et al. 2006b, *MNRAS*, 373, L45
- Dobbie, P. D., Day-Jones, A., Williams, K. A., et al. 2012, *MNRAS*, 423, 2815
- Fellhauer, M., Lin, D. N. C., Bolte, M., Aarseth, S. J., & Williams, K. A. 2003, *ApJ*, 595, L53
- Fernie, J. D. 1963, *AJ*, 68, 780
- Fontaine, G., Brassard, P., & Bergeron, P. 2001, *PASP*, 113, 409
- Garcia-Berro, E., Isern, J., & Hernanz, M. 1997, *MNRAS*, 289, 973
- Gianninas, A., Bergeron, P., & Ruiz, M. T. 2011, *ApJ*, 743, 138
- Kalirai, J. S., Ventura, P., Richer, H. B., et al. 2001, *AJ*, 122, 3239
- Kalirai, J. S., Richer, H. B., Reitzel, D., et al. 2005, *ApJ*, 618, L123
- Kalirai, J. S., Bergeron, P., Hansen, B. M. S., et al. 2007, *ApJ*, 671, 748
- Kalirai, J. S., Hansen, B. M. S., Kelson, D. D., et al. 2008, *ApJ*, 676, 594
- Kalirai, J. S., Saul Davis, D., Richer, H. B., et al. 2009, *ApJ*, 705, 408
- Kepler, S. O., Pelisoli, I., Koester, D., et al. 2016, *MNRAS*, 455, 3413
- Kleinman, S. J., Kepler, S. O., Koester, D., et al. 2013, *ApJS*, 204, 5
- Koester, D., & Kepler, S. O. 2015, *A&A*, 583, A86
- Liebert, J., Young, P. A., Arnett, D., Holberg, J. B., & Williams, K. A. 2005, *ApJ*, 630, L69
- Oke, J. B., Cohen, J. G., Carr, M., et al. 1995, *PASP*, 107, 375
- Raddi, R., Catalán, S., Gänsicke, B. T., et al. 2016, *MNRAS*, 457, 1988
- Rubin, K. H. R., Williams, K. A., Bolte, M., & Koester, D. 2008, *AJ*, 135, 2163
- Tremblay, P.-E., Bergeron, P., & Dupuis, J. 2009, *Journal of Physics Conference Series*, 172, 012046
- Tremblay, P.-E., Bergeron, P., & Gianninas, A. 2011, *ApJ*, 730, 128
- Tremblay, P.-E., Schilbach, E., Röser, S., et al. 2012, *A&A*, 547, A99
- Williams, K. A., Bolte, M., & Koester, D. 2004, *ApJ*, 615, L49
- Williams, K. A., & Bolte, M. 2007, *AJ*, 133, 1490
- Williams, K. A., Bolte, M., & Koester, D. 2009, *ApJ*, 693, 355